

# Ion and electron generation by laser useful for radiotherapy and adrontherapy

A. Lorusso<sup>(1)</sup>, M.V. Siciliano<sup>(1),(3)</sup>, L. Velardi<sup>(1),(2)</sup> and V. Nassisi<sup>(1)</sup>

<sup>(1)</sup>Laboratorio di Elettronica Applicata e Strumentazione LEAS, Department of Physics, University of Salento - Lecce, Via Provinciale Lecce-Monteroni, 73100 Lecce – Italy, Tel. +39 0832 297495, Fax. +39 0832 297482,

E-Mail: [vincenzo.nassisi@le.infn.it](mailto:vincenzo.nassisi@le.infn.it)

<sup>(2)</sup>Department of Physics, University of Bari, Via Amendola, 70126 Bari – Italy

<sup>(3)</sup>Department of Material Science, University of Salento, Via Provinciale Lecce-Monteroni, 73100 Lecce – Italy

## Abstract

Laser beams can be utilized to produce ions and electrons to be applied in radiotherapy and adrontherapy. We describe the innovative techniques to extract ions and electrons from plasma provided by metal target of different elements and electron of low emittance by photoelectric effect. Beside, the characterization of beams consists in the measurements of electromagnetic and geometric properties. The technique very used to get geometric properties is the pepper pot or double slit. By measurements the emittance values obtained were very low pointing out the laser application in particles generation is a very interesting means to produce low emittance beams.

## INTRODUCTION

High intensity ion or/and electron beams of moderate energy and good geometric qualities are more and more utilised in biomaterial modifications [1], nuclear physics experiments [2], innovative electronic materials fabrication [3], hadrontherapy applications [4], new radio-pharmacy researches [5, 6], free-electron lasers (FEL) devises [7], X-ray machines devises [8], high power microwave generators development [9], thermonuclear fusion reactors control [10].

The interaction of laser beams can generate plasma composed by positive, negative and neutral particles if the laser intensity is high. It is possible to get only electrons if their intensity is very low. This last effect is called photoelectric process. We also will detail the techniques to get ion-acoustic waves.

## CHARGE GENERATED BY LASER PLASMA

Today, the most usual methods to generate ions is the application of electron beams directed on

solid target which etches the material. A method more complex is the electron cyclotron resonance applied to gases. This last method applied to solid elements needs to have material previously evaporated [11]. We present the pulsed laser ablation technique from solid target to obtain energetic ions and electrons whose energy can be further increased by successive acceleration [12-16].

The development of intense laser beams if applied on metal target can generate laser-induced plasma [12]. This innovative technique is very important because it can generate beams also from refractory materials [17].

The plasma is well known as an ionized gas formed by electrons, ions, atoms, molecules and clusters. By the use of electric field it is possible to extract specific charged particles. This idea must be applied to plasmas of moderate density owing to their low conductivity. In fact, a very dense plasma becomes good conductor such as a metal and electric fields provoke breakdowns. Breakdowns are also influenced by the value of the particle energy. In fact, high energy particles do not lead the electric field directions and they can inhibit the breakdowns. Therefore, to extract charged component it is necessary to choose very low density plasmas in order to overcome the conducting phase and breakdowns.

To produce plasma we focus a laser beam onto a target surface obtaining material ablation.

By the above apparatus it is possible to get positive and negative particles depending by the Faraday cup bias. The electric circuit for the cup utilized in this experiment is drawn in Fig. 2.

Typical example of ion signal by  $-300$  V bias voltage and electron signal by  $+300$  V bias voltage is showed in Fig. 3.

The signal of Fig. 3 are obtained by a Ge target irradiated by KrF laser beam. It is noteworthy that both signals have the same on set-time indicating that the plasma is a very compact fluid and it is possible to separate by the application of a electric

field. Often if very energetic particles are present they can escape from the plume.

### ION GENERATION

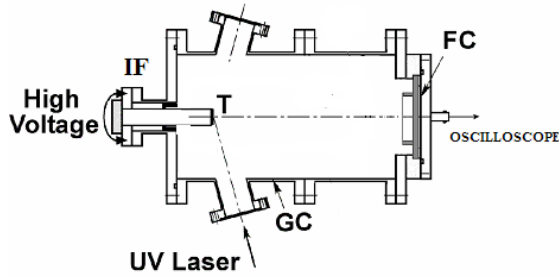


Fig. 1. Experimental apparatus. T: target; FC: Faraday cup; GC: ground chamber.

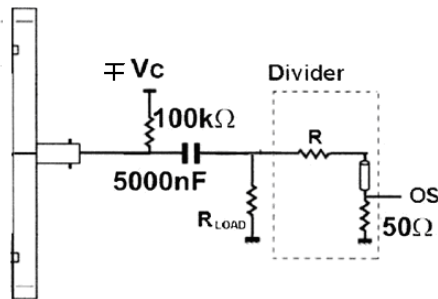


Fig. 2. Electric schema to polarize the Faraday cup.  $-V_c$  is applied to collect positive ions;  $+V_c$  is applied to collect negative charges.

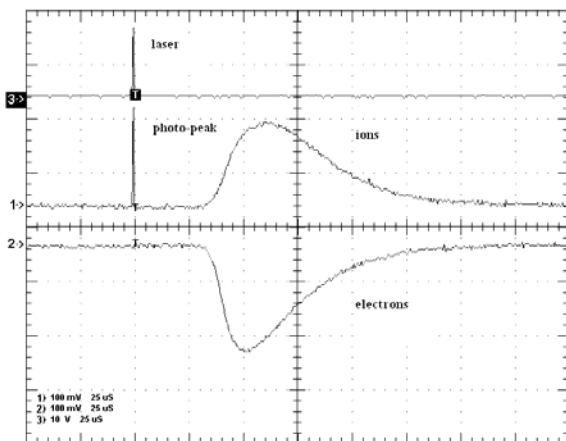


Fig. 3. Waveform of an ion and an electron beam.

To get accelerated ions we used a KrF excimer laser, operating at 248 nm wavelength (5 eV photon energy), 25 ns pulse duration and a vacuum chamber made of stainless steel. The vacuum chamber was evacuated by two turbo-molecular pumps down to  $10^{-6}$  mbar. Our accelerator consisted of a plasma expanding chamber (EC) which allows an initial free expansion of the plasma before the

ion extraction contained into the accelerator chamber(GC). The target support was a stem of 2 cm in diameter mounted on an insulating flange kept to positive high voltage, in DC mode. A grounded electrode (GE) in front to the expanding chamber allowed either to generate an intense electric field or to support the substrate to be processed. The expanding chamber was indispensable to avoid arcs and to apply accelerating voltages up to 80 kV. It must be hermetic in order to contain the plasma around target otherwise imperceptible losses generate short circuits.

The laser beam enters into the implantation chamber at an angle of  $70^\circ$  with respect to the normal to the target (T) surface, through a thin quartz window by a focusing lens forming a spot of less than  $0.01 \text{ cm}^2$  on the surface of the target. Fig. 4 shows the sketch.

By this method the percentage of ionization of the ablate material is not very high but sufficient

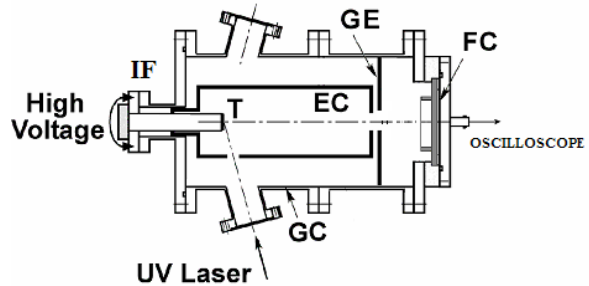


Fig. 4. Experimental apparatus. T: target; FC: Faraday cup; GE: ground electrode; GC: ground chamber; EC: expansion chamber. IF: insulating flange.

to get ion beams of high intensity. The percentage of the ionized material is about 16% near the target with respect to the total ablated material, due to the absorbed energy via bremsstrahlung. The plume temperature recorded can get values of hundred thousand Kelvin[15, 18]. Besides, the total beam energy depends by the voltage applied and by the charge state of the particles. The maximum value of

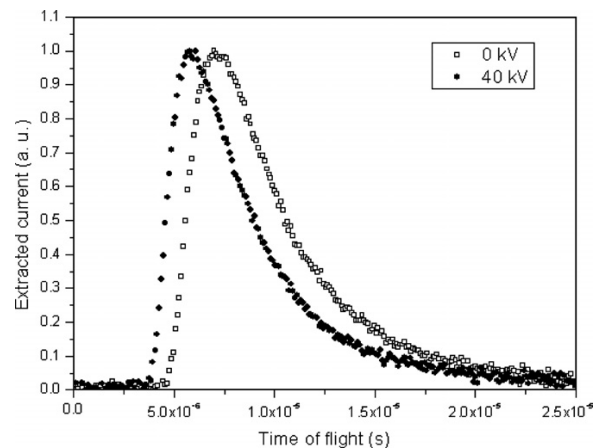


Fig. 5. Waveform of an ion beams of Cu under and without the accelerating voltage of 40 kV.

the accelerating voltage is mainly dependent on the chamber volume and its morphology. Using different metallic targets we obtained different ion beams. It is noteworthy observe that applying the accelerating voltage the ions are accelerated and the current signal becomes anticipate, Fig. 5.

If we want to increase the acceleration it is necessary to maximize the acceleration area, so it corresponds to applying a negative voltage to the cup collector. Fig. 6 shows a new apparatus.

The preliminary measurements were performed by a copper target at 9 mJ laser energy. Fig.

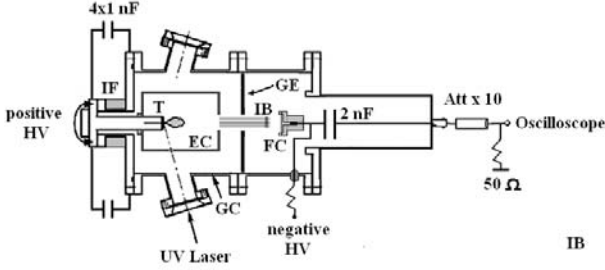


Fig. 6. Experimental apparatus containing double acceleration system.

7 shows the time of fly waveforms at different accelerating voltage. Again in this case it is noteworthy observe that the ion current peak anticipates with accelerating voltage.

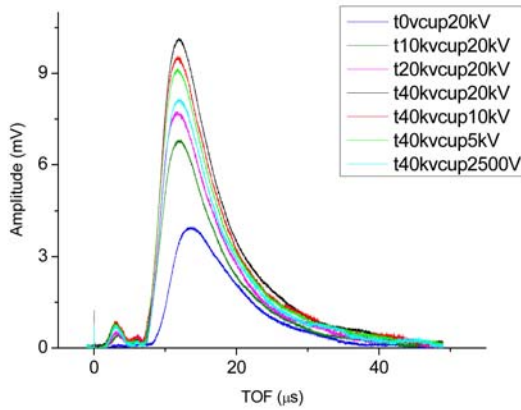


Fig. 7. Waveform of an ion beams of Cu under the accelerating voltage applied to the target and cup.

At fast time scale we can observe small peaks we can ascribed to light ion (p, C and O) that escape the plasma plume.

In this case the plasma is governed by the shifted Maxwell-Boltzmann distribution (MBD):

$$f_{KL}(v_x, v_y, v_z, E) \propto \exp\left[-\frac{2E + m(v_x - v_d)^2}{2kT}\right] \cdot \exp\left[-m\frac{v_y^2 + v_z^2}{2kT}\right] \quad (1)$$

and the current will be:

$$j_{IC}(L, t) \propto t^{-5} \exp[-\beta^2(L/t - u)^2] \quad (2)$$

where,  $L$  is the target-cup distance,  $v_d$  is the centre-of-mass velocity and  $\beta^2 = m/2kT$ ,  $m$  is the mass of ion,  $k$  is the Boltzmann constant and  $T$  is related to the ion temperature. By the fit it is possible to get the  $v_d$  and temperature of the beam.

## ELECTRON GENERATION (ion-acoustic waves)

During our experiments we wanted to extract electrons from a small area and for this reason we placed a disk having a hole of about 1 cm in diameter in front the plasma flux, Fig. 8. Polarizing positively the cup collector we detected special signals [19].

On the contrary to the signal obtained previ-

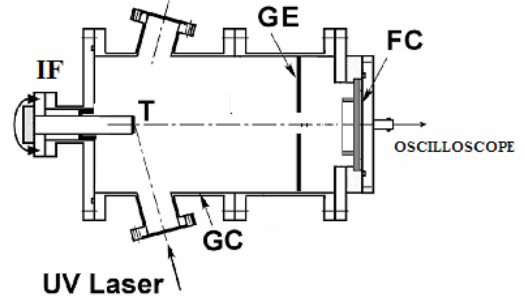


Fig. 8. Experimental apparatus. T: target; FC: Faraday cup; GC: ground chamber.

ously and showed in Fig. 3, we observed a negative signal due to the electron polarity but with many oscillations. This behavior was very interesting because it was not observed in previous. Fig. 9 shows the experiment result for a Ge target and the Faraday cup polarized at + 300V.

In this case, the ions feeling the repulsive potential, are slowed down in proximity of the hole.

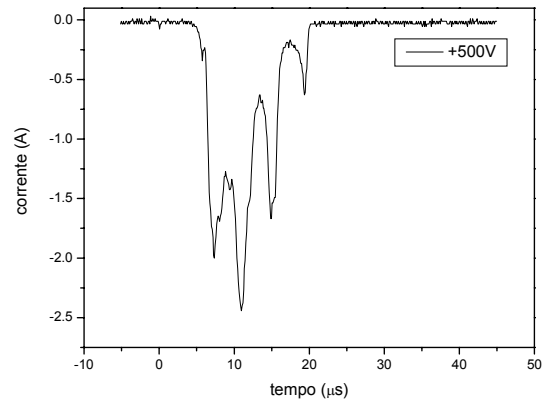


Fig. 9. Waveform of an electron beam modulated.

Instead, the electrons are torn away from the plasma edge, due to their high mobility. As a consequence, an excess of positive charge in comparison with the column of plasma will grow near the EC hole. The ions will therefore form regions of compression and rarefaction, priming oscillations in the density distributions of ions and electrons and in the electric field longitudinal component.

From a quantitative point of view, we can state that the plasma propagates in a field with cylindrical symmetry, coaxial to the EC circular hole. Such a field has an analytical expression in the approximation in which the EC walls (potential at zero) are located at an infinite distance from the hole. Assuming that such approximation is valid in proximity of the symmetry axis, it is possible to deduce the following formula for the electric potential,  $\phi$ , near the hole,

$$\phi = \frac{E_0 a}{\pi} \left[ 1 - \frac{z}{a} \operatorname{arctg} \frac{a}{z} \right] \quad (3)$$

Solving we have oscillations of frequency:

$$\omega_s = kv_s = \frac{\pi}{L} nv_s \quad (4)$$

where  $v_s$  is the sound velocity in the plasma plume given by the following relation:

$$v_s = \sqrt{\frac{\gamma k_B T_i}{M}} \quad (5)$$

where  $T_i$  is the ion temperature,  $M$  is the ion mass,  $\gamma$  the Mayer factor ( $\gamma = 5/3$ ) and  $k_B$  is the Boltzmann constant. The following oscillations are due to ion-acoustic waves. These results are interesting because open new methods in radiofrequency generation.

## PHOTOELECTRIC EFFECT

The important advantage of photo-cathodes is their possibility in producing electron beams whose intensity, duration and emittance can be easily controlled by suitable choice of the laser source and target work function, as one can see in the theory sect. Besides, the cathode materials are not expensive, they have a long life time and can work at moderate vacuum levels. Again, the high voltage utilized in order to extract and to accelerate the electrons has not to be necessary pulsed, i.e. synchronized with the laser pulse, but a direct current high voltage applied to the cathode will be sufficient.

## Theory

The more general laser-generated electron emission from metal surfaces is governed by the modified Fowler-DuBridge equation by Bloembergen and Bechtel [20], containing the current terms:

$$J = \sum_{n=0}^{N+1} J_n \quad (6)$$

with

$$J_n(t) = a_n AI^n(t)(1-R)^n T^2(t) F(\delta_n) \quad (7)$$

where  $I$  is the incident laser power,  $R$  is the target optical reflection,  $A/(K^2 \cdot \text{cm}^2)$  is Richardson constant,  $T$  is the target temperature,  $F(\delta_n)$  is the Fowler function of argument  $\delta_n = (nh\nu - \phi)/kT$ ,  $a_n$  are the quantum coefficients (with  $a_0=1$ ) related to the quantum  $n$ -photon process, with  $0 \leq n \leq N+1$ , where  $N$  is the first integer number below to the ratio  $\phi/h\nu$ .  $\phi$  is the metal surface work function and  $h\nu$  is the photon energy.

For  $h\nu > \phi$ , by the theory, the emission has only two terms, namely, for  $N=0$ :

$$J_0 = AT^2 \exp(-\phi/kT) \quad (8)$$

and for  $N=1$

$$J_1 \cong a_1 AI(t) T^2 (1-R) \times \left[ \frac{1}{2} \left( \frac{h\nu - \phi}{kT} \right)^2 + \frac{\pi^2}{6} \right] \quad (9)$$

The thermionic component will be negligible because the maximum temperature reaching in this experiment is few hundreds of  $K$  and the thermionic component is negligible with respect the total current [21].

## EXPERIMENTS

Fig. 10 shows a sketch of the apparatus. A 100 cm focal length lens (L) is utilized to lead the beam onto the target (T). A beam splitter (B) is used to send part of the laser beam to a photodiode (Ph) in order to control its waveform. The photoelectric charge measurements are performed in a vacuum stainless-steel chamber connected to turbomolecular pump, the vacuum in this case reached during the experiments was of about  $10^{-8}$  mbar. The cathodes are disks of pure zinc, yttrium, copper, ect.

The distance anode-cathode is set to  $d=5$  mm. The extremity of the cathode is connected to the ground by a shunt composed of 15 resistors ap-

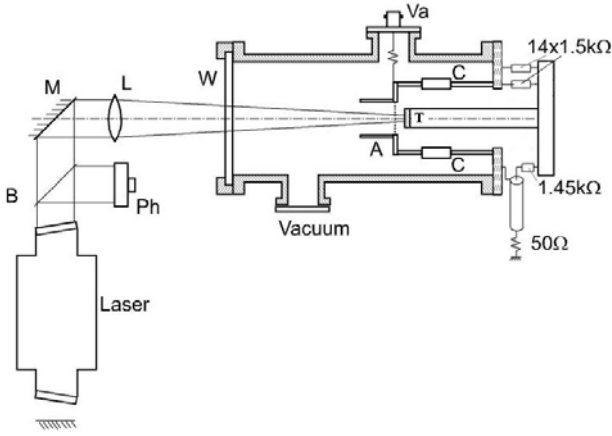


Fig. 10. Experimental apparatus. M: mirror; B: beam splitter; Ph: photodiode; L: Lens; Va: high voltage; T: Target; A: anode; C: capacitors.

proximately of  $1500 \Omega$  connected in parallel. This configuration is able to match the signal. Four capacitor of  $350 \text{ pF}/40 \text{ kV}$  are used to stabilize the voltage. The anode is made by a stainless steel grid with 4 meshes per  $\text{mm}^2$ , presenting an optical transmittance of 64%.

Typical waveform of the laser and current pulses for a cathode of Y with a laser energy of 16 mJ is shown in Fig. 11. It is possible to note that both time duration are very similar pointing out that by this method one can have electron beams of controlled width. Beside the output current can be controlled by Child-Langmuir (CL) law, in fact the current density is  $j=2.43 \times 10^{-6} Va^{3/2}/d^2$ . The experimental results for different laser energies are pictured in Fig. 12.

We can observe that the peak current increases with the laser energy and accelerating voltage, at low values. At high accelerating voltage the current reaches the saturation regime, while at low ones overcomes the CL values. This last behavior is

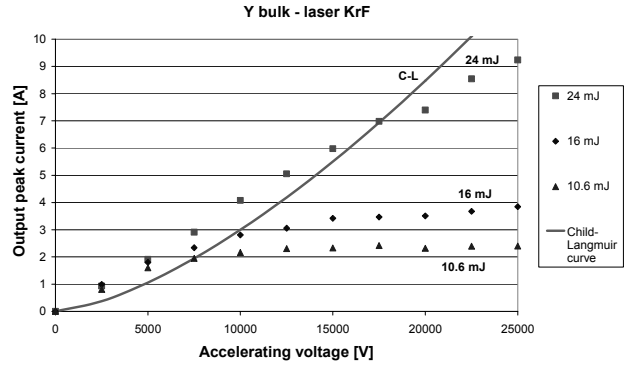


Fig. 12. Experimental results of electron emission on accelerating voltage at different laser energy values.

ascribed to the plasma formation generally present during the electron beam formation that we associate an impedance  $Z$ . The output current will be governed by :

$$i = 2.43 \times 10^{-6} S \frac{(V - Zi)^{3/2}}{(d - vt)^2} \quad (10)$$

In this experiment we obtained quantum efficiencies more than  $10^{-4}$ .

### EMITTANCE

To evaluate the geometric characteristics of the beam we measured the emittance value by the pepper pot method. Let me define the area of the particle in the phase space as:

$$A_x^o = \iint_{f_2^o \neq 0} dx dp_x = p_z A_x \quad (11)$$

Where  $f_2^o$  is the distribution function of the parti-

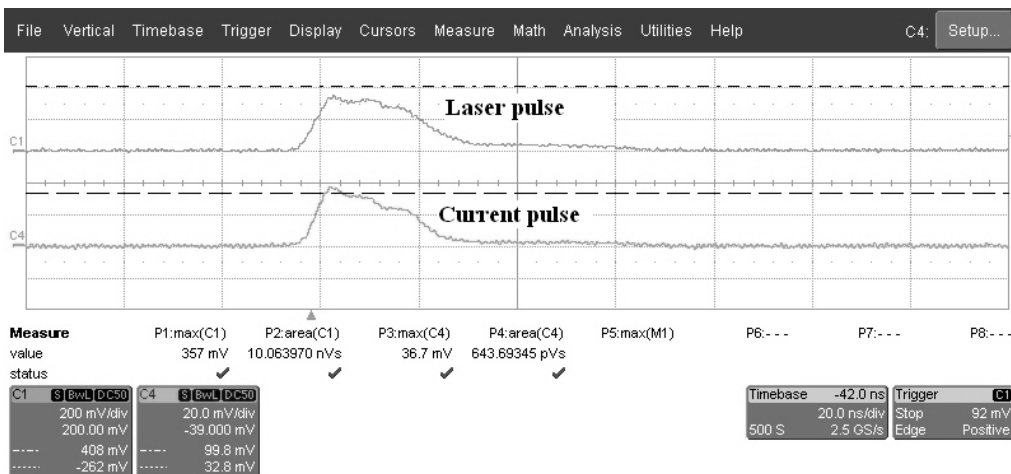


Fig. 11. Experimental results. Waveform of laser and electrons at 16 mJ, 20 kV accelerating voltage.

cles,  $p_z$  is the moment along the propagation axis and  $A_x$  is the area occupied by the particles in the trace space.  $p_z$  is linked to  $p_x$  by the following relation:  $p_x = p_z dx/dz$ .

Substituting the expression of  $p_z = m_o c \beta \gamma$  in the Eq. 11, we have:

$$A_x^o = m_o c \beta \gamma A_x \quad (12)$$

where  $m_o$  is the rest mass of the particles and  $\beta = v/c$  and  $\gamma = 1/(1-\beta^2)^{1/2}$ .

Generally the beam is accelerated and  $p_z$  is not constant, then it is necessary to define an invariant quantity called *normalized emittance* in the trace plane  $xx'$ :

$$\varepsilon_{nx} = \beta \gamma \varepsilon_x \quad (13)$$

and in the trace plane  $yy'$ :

$$\varepsilon_{ny} = \beta \gamma \varepsilon_y \quad (14)$$

By the above considerations to get low emittance beams it is necessary to have a low transversal spread energy. This points out that for thermionic emission the  $kT$  value must be low while for photoelectric emission  $nh\nu - \phi$  must be low, namely:

$$\varepsilon_{max} = \frac{r}{2} \sqrt{\frac{kT}{m\dot{c}^2}} = \frac{r}{2} \sqrt{\frac{nh\nu - \phi}{m\dot{c}^2}} \quad (15)$$

$\varepsilon_{max}$  represents the upper limit of emittance.

### Ion beam emittance

To evaluate the emittance of the ion beam we exploit the pepper pot method. This method consists in a mask of small holes to select the beam and a screen to determinate the divergence. The mask has 5 holes of 1 mm in diameter and it is fixed on the GE of Fig. 6. Fig. 13 shows the photo of the used mask. As screen we utilise a PVC disk placed behind the mask at a distance of 2 cm. The ion beam imprinted the PVC and then it is possible to measure the divergence.

We applied 50000 ion shots to evidence the transversal dimensions of the beam. Fig. 14 shows the sketch and 15 the area of the beam in the trace plane. From this last figure the emittance value found resulted of 0.22 p mm mrad. At moment the above measurement is rather rough but very interesting.

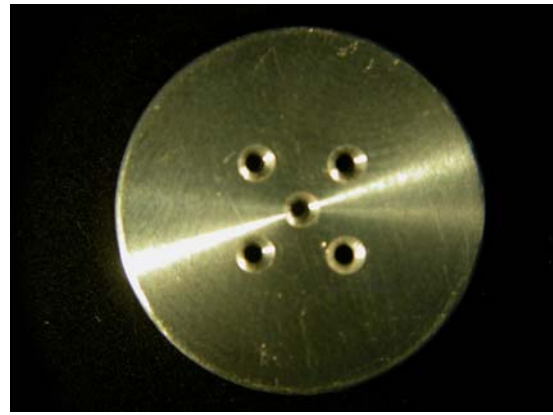


Fig. 13. Photo of mask having 5 holes of 1 mm in diameter.

### Electron beam emittance

The first approach we utilized to measure the emittance was the double slit. Generally more pairs of double slits are used. The slits are mobile in order to select the direction of the beamlet choice. An sketch of the apparatus is shows in Fig. 16. The

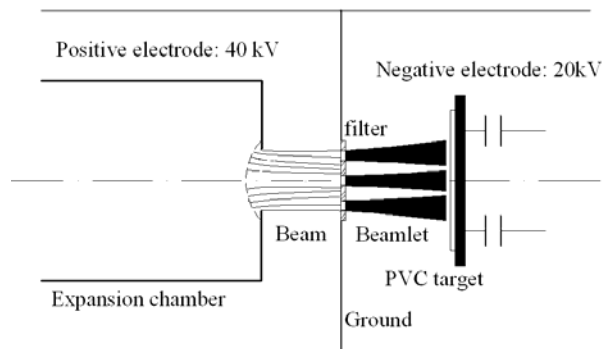


Fig. 14. Diagram of the pepper pot schema.

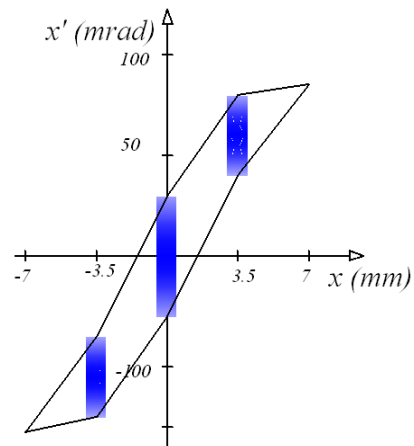


Fig. 15. Emittance diagram in the trace plane.

laser beam illuminates an very small area of the target connected to negative voltage,  $-HV$ .

By this method the slits are mobile and their position determines the beamlet direction. The cups record the current on direction. If we consider the total current we obtain a large emittance, instead if we consider the direction in corresponding of the

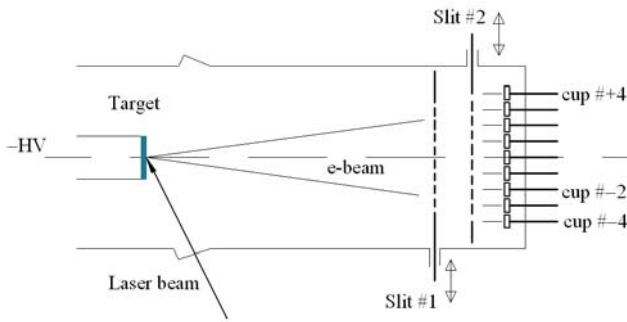


Fig. 15. Experimental apparatus to measure e-beam emittance.

only current higher than 50% we obtain a lower emittance. Fig. 16b shows an example of the beam in the trace plane and the emittance at different levels. We can observe that only at the 80% of the total current we have a low emittance.

The current obtained utilizing an KrCl laser and an copper target was 370 at 50 kV accelerating voltage with a normalized emittance of  $9 \pi$  mm rad.

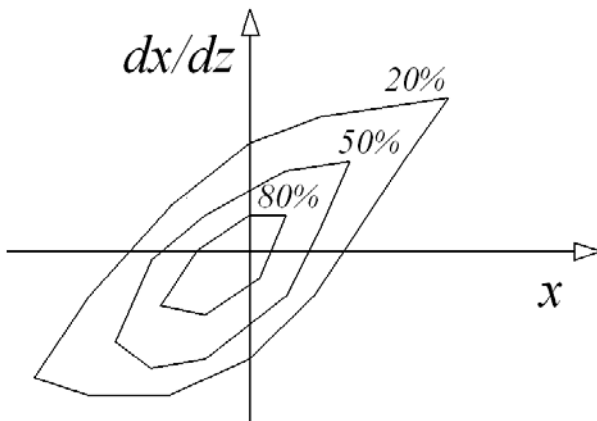


Fig. 16. Emittance diagram in the trace plane of an electron beam.

**CONCLUSION**

We have demonstrated that lasers are very important means to get particles. The particles can feed large accelerators utilised for medical application and material processing. The emittance values measured are very low and this can assure an high efficient in coupling the sources with accelerators.

**REFERENCES**

[1] A. Lorusso, L. Velardi, V. Nassisi, L. Torrissi, D. Margarone, A. Mezzasalma and A.

Rainò, Rad. Eff. Def. Solids 163 (2008).  
 [2] E. Amaldi, E. Fermi e F. Rasetti, "La Ricerca Scientifica 40, ser. II (1937).  
 [3] A. Lorusso, V. Nassisi, L. Velardi, G. Congedo, Nucl. Instrum. Meth. B 266, 2486-89 (2008).  
 [4] L. Picardi et al. Proc. EPAC '94, p. 864 (1994).  
 [5] H. Takeda, J.H. Billen, S. Nath, J.E. Stoval, R.L. Wood, L.M. Young. Proc. IEEE Part. Accel. Conf. 2, 1140 (1995).  
 [6] M.A. Fortin, F. Marion, B.L. Stansfield, R.W. Paynter, A. Sarkissian, B. Terreault, ad Surf. and Coatings Technology, 200, 996 (2005).  
 [7] Y. Kawamura, K. Toyoda and M. Kawai, Appl. Phys. Lett. 45, 307 (1984).  
 [8] C. S. Campos, M. A. Z. Vasconcellos, X. Llovet and F. Salvat, Phys. Rev. A 66, 127191 (2002).  
 [9] J. A. Nation, Appl. Phys. Lett. 21, 491 (1970).  
 [10] L. S. Levine and I. M. Vitkovitsky, IEEE Trans. NS-18, 255 (1971)  
 [11] F. Bourg et al. Nucl. Instrum. Methods. Phys. Res. A254, 13 (1987).  
 [12] A. Luches, M. Martino, V. Nassisi, A. Pecoraro and A. Perrone, Nucl. Instrum. Methods. Phys. Res. A322, 166 (1992).  
 [13] A. Beloglazov, V. Nassisi, M. Primavera, Rev. Sci. Instrum. 66, 3883 (1995).  
 [14] V. Nassisi and A. Pedone, Rev. Sci. Instrum. 74, 68 (2003).  
 [15] D. Doria, A. Lorusso, F. Belloni, and V. Nassisi, Rev. Sci. Instrum, 75, 4763 (2004).  
 [16] D. Bleiner, A. Bogaerts, F. Belloni and V. Nassisi, Appl. Phys. 101, 83301 (2007).  
 [17] A. Lorusso, L. Velardi, V. Nassisi, F. Paladini, A. M. Visco, N. Campo, L. Torrissi, D. Margarone, L. Giuffrida, A. Rainò, Nucl. Instrum. Meth. B266, 2490 (2008).  
 [18] L. La'ska, J. Kra'sa, K. Masek, M. Pfeifer, K. Rohlena, B. Kra'likova', J. Ska'la, E. Woryna, P. Parys, J. Wolowski, W. Mro'z, B. Sharkov, and H. Haseroth, Rev. Sci. Instrum. 71, 927 (2000).  
 [19] L. Marra, F. Belloni, A. Lorusso, V. Nassisi and L. Martina, REDS 160, 621 (2005)  
 [20] J.H. Bechtel, W. Lee Smith, N. Bloembergen, Phys. Rev. B 15, 4557 (1977).  
 [21] V. Nassisi and F. Paladini, Appl. Phys. B 71, 1-4 (2000).